A novel mechanism for imatinib mesylate–induced cell death of BCR-ABL–positive human leukemic cells: caspase-independent, necrosis-like programmed cell death mediated by serine protease activity

Masayuki Okada, Souichi Adachi, Tsuyoshi Imai, Ken-ichiro Watanabe, Shin-ya Toyokuni, Masaki Ueno, Antonis S. Zervos, Guido Kroemer, and Tatsutoshi Nakahata

Caspase-independent programmed cell death can exhibit either an apoptosis-like or a necrosis-like morphology. The ABL kinase inhibitor, imatinib mesylate, has been reported to induce apoptosis of BCR-ABL–positive cells in a caspase-dependent fashion. We investigated whether caspases alone were the mediators of imatinib mesylate–induced cell death. In contrast to previous reports, we found that a broad caspase inhibitor, zVAD-fmk, failed to prevent the death of imatinib mesylate–treated BCR-ABL–positive human leukemic cells. Moreover, zVAD-fmk–preincubated, imatinib mesylate–treated cells exhibited a necrosis-like morphology characterized by cellular pyknosis, cytoplasmic vacuolization, and the absence of nuclear signs of apoptosis. These cells manifested a loss of the mitochondrial transmembrane potential, indicating the mitochondrial involvement in this caspase-independent necrosis. We excluded the participation of several mitochondrial factors possibly involved in caspase-independent cell death such as apoptosis-inducing factor, endonuclease G, and reactive oxygen species. However, we observed the mitochondrial release of the serine protease Omi/HtrA2 into the cytosol of the cells treated with imatinib mesylate or zVAD-fmk plus imatinib mesylate. Furthermore, serine protease inhibitors prevented the caspase-independent necrosis. Taken together, our results suggest that imatinib mesylate induces a caspase-independent, necrosis-like programmed cell death mediated by the serine protease activity of Omi/HtrA2. (Blood. 2004;103:2299-2307)

© 2004 by The American Society of Hematology

Introduction

Imatinib mesylate (imatinib, Gleevec) was developed as a potent and specific inhibitor of ABL tyrosine kinase.[1] Preclinical studies and clinical trials showed that imatinib exhibited a remarkable single-agent activity against BCR-ABL–expressing cells with acceptable toxicity in vitro and in vivo.[1,2] BCR-ABL tyrosine kinase activates several signaling pathways such as the Ras/mitogen-activated protein kinase,[2-4] signal transducer and activator of transcription 5,[2,4] and phosphatidylinositol 3 kinase/Akt pathways[2,4]; enhances nuclear factor κB (NF-κB) activity[5]; up-regulates the level of Bcl-X$_L$[5,6]; and suppresses the mitochondrial apoptotic pathway.[5,7] Imatinib counteracts BCR-ABL tyrosine kinase and induces apoptosis in BCR-ABL–positive cells[8-10] in a caspase-dependent fashion.[11,12] Recently, however, it has been revealed that responses to imatinib are not necessarily remarkable or durable in some patients with BCR-ABL–positive leukemia,[13-22] and thus an increasing number of studies have searched for a novel therapy targeting the BCR-ABL–induced signaling pathways.[5]

Cell death is generally classified into 2 categories, apoptosis[23,24] and necrosis. Apoptosis is a well-documented active programmed cell death (PCD) in which the activation of caspases plays a central role.[25] In contrast, necrosis has been conceived as a passive cell death without established regulatory mechanisms. However, it has recently been reported that necrosis-like cell death may be regulated by cellular intrinsic death programs.[26-28] This active necrosis-like PCD is observed in various paradigms of cell death in conditions in which caspases are inhibited.[26,27] Indeed, there is increasing evidence for caspase-independent cell death,[29] and caspase inhibition occasionally turns the morphology of PCD from apoptosis into necrosis without inhibiting death itself.[26,30,31] Although these models of caspase-independent necrosis might provide potential targets for a novel cancer therapy, little or no information is available on their signaling pathways.

There are 2 well-established pathways that lead to cell death, the death-receptor pathway and the mitochondrial pathway.[25] In particular, the mitochondrial pathway is used extensively in response to various extracellular and intracellular insults. Mitochondria play a pivotal role in the induction of cell death by releasing several proteins localized in the intermembrane space.[32] Among these proteins, cytochrome c and Smac/DIABLO function as caspase activators, while apoptosis-inducing factor (AIF)[33] and endonuclease G (Endo G) can mediate caspase-independent cell death.[29] Omi/HtrA2, another intermembrane protein, plays a dual

role as a caspase activator (acting as an inhibitor of the inhibitor of apoptosis [IAP] proteins) and as a caspase-independent death effector (acting by virtue of its serine protease activity). Overproduction of reactive oxygen species (ROS) resulting from a dysfunction in the mitochondrial respiratory chain may also lead to caspase-independent cell death.[34]

In the present study, we show that a broad caspase inhibitor, zVAD-fmk (zVAD), fails to prevent the imatinib-induced cell death in BCR-ABL–positive human leukemic cells, that this zVAD + imatinib–induced cell death exhibits a necrosis-like morphology accompanied by the cytosolic release of Omi/HtrA2, and that this caspase-independent necrosis is prevented by serine protease inhibitors. Our results suggest that imatinib induces a caspase-independent, necrosis-like PCD in BCR-ABL–positive human leukemic cells, which is mediated by the serine protease activity of Omi/HtrA2.

Materials and methods

Cells

BV173 was kindly provided by Dr Matsuo (Hiroshima University, Japan) and K562 was purchased from RIKEN Gene Bank (Tsukuba, Japan). BV173 is an established human leukemic cell line derived from a patient with chronic myelogenous leukemia (CML) lymphoid blastic crisis, and K562 is derived from a patient with CML erythroid blastic crisis. Cells were maintained in RPMI1640 (Sigma, St Louis, MO) supplemented with 10% heat-inactivated fetal bovine serum (FBS; JRH Biosciences, Lenexa, KS) in the absence of antibiotics at 37°C under 5% CO_2. Exponentially growing cells were used throughout all experiments at a concentration of 0.2 to 1.0×10^6 cells/mL.

Reagents

Imatinib was kindly provided by Novartis Pharma (Basel, Switzerland). zVAD was from Peptide Institute (Osaka, Japan). Serine protease inhibitors, N-a-tosyl-L-lysine-chloromethyl ketone (TLCK) and L-I-p-tosylamino-2-phenylethylchlorome ketone (TPCK), were from Research Organics (Cleveland, OH). All these reagents were dissolved in dimethyl sulfoxide (DMSO; Nacalai Tesque, Kyoto, Japan) and stored at −20°C. The concentration of DMSO as vehicle control was kept under 0.1% throughout all experiments to avoid cytotoxic effects. Other reagents were used at the following concentrations: zVAD, 40 μM, imatinib, 1 μM; TPCK, 25 μM (BV173) or 50 μM (K562), and TLCK, 100 μM (BV173) or 200 μM (K562). For combination of zVAD and imatinib (zVAD + imatinib), cells were preincubated with zVAD for 90 minutes and thereafter treated with imatinib. For combination of TLCK (or TPCK), zVAD, and imatinib (TLCK [or TPCK] + zVAD + imatinib), cells were preincubated with TLCK (or TPCK) and zVAD for 90 minutes and then treated with imatinib. Staurosporine (STS) was purchased from Sigma; 3,3′-dihexyloxacarbocyanine iodide (DiOC6(3)), propidium iodide (PI), and 2′,7′-dichlorofluorescein-diacetate (DCFH-DA) were purchased from Molecular Probes (Eugene, OR).

Cell death assessment and determination of mitochondrial transmembrane potential (ΔΨm)

Cell death was defined by PI staining, and mitochondrial transmembrane potential (ΔΨm) was determined by DiOC6(3). For each condition, 0.5 to 1.0×10^6 cells/mL were incubated with 40 nM DiOC6(3) and 5 μg/mL PI at 37°C for 15 minutes, and subsequently their fluorescence was measured using FL1 and FL3 channels of FACSCalibur (Becton Dickinson, Franklin Lakes, NJ).

Morphologic evaluation by light and electron microscopy

After treatment, 2 to 3×10^4 cells were spun down onto slides with cytospin, stained with Diff-Quick (International Reagents, Kobe, Japan),

and subsequently examined by light microscopy for morphologic evaluation. A minimum of 400 cells was scored for each sample, and the percentage of each morphologic type was determined.

For the observation by transmission electron microscopy, 5×10^7 treated cells were spun down into pellet, fixed in 2% glutaraldehyde in 0.1 M phosphate buffer at 4°C, washed in isotonic phosphate-buffered sucrose solution, refixed in phosphate-buffered 1% osmium tetroxide solution, dehydrated in a graded series of ethanol, and embedded in Luveak 812 (Nacalai). Sections were cut 70- to 90-nm thick with a diamond knife on a Sorvall MT-5000 ultramicrotome (Kendro, Newtown, CT), stained with uranyl acetate and lead citrate, and observed with a Hitachi H-7000 electron microscope (Hitachi, Tokyo, Japan).

Assessment of internucleosomal DNA fragmentation and DNA content

For internucleosomal DNA fragmentation assay, DNA was extracted using ApopLadder Ex (Takara, Shiga, Japan) according to the manufacturer's instructions. In brief, DNA extract from 3×10^5 cells treated under each condition was dissolved with 50 μL TE buffer (pH 8.0; Nacalai) and electrophoretically resolved in a 2% agarose gel. After incubation of the gel in distilled water containing 0.5 μg/mL ethidium bromide for 30 minutes, fragmented DNA was visualized under ultraviolet light.

DNA content was assessed by flow cytometry. Cell permeabilization and staining with PI have been described elsewhere.[35] Briefly, after treatment, 0.5 to 1.0×10^6 cells were washed, fixed with 4 mL ice-cold 95% ethanol added dropwise during continuous vortexing, and incubated on ice overnight. Cells were resuspended in 1 mL 1% bovine serum albumin (BSA; Sigma)–phosphate-buffered saline (PBS) and washed and treated with 0.25% Triton X-100 (Nacalai) for 5 minutes. Cells were then washed 3 times with 1% BSA-PBS. DNA was stained with 500 μL 1% BSA-PBS, 100 μg/mL RNase A (Sigma), and 20 μg/mL PI. Nuclear emitted fluorescence was measured by FACSCalibur, and the percentage of the sub-G_1 fraction was determined using ModFit LT 2.0. (Verity Software, Topsham, ME).

Caspase activity assay

For caspase activity assay, the procedure was performed using the Caspase Fluorometric Protease Assay Kit (MBL, Nagoya, Japan) according to the manufacturer's instructions. Briefly, cell lysate from 1.0×10^6 cells was incubated at 37°C for 1 hour with 50 μM DEVD-AFC, IETD-AFC, and LEHD-AFC substrate to measure caspase-3, -8, and -9 activity, respectively. AFC fluorescence was determined (excitation, 390 nm; emission, 510 nm) with the Wallac ARVO SX$_{FL}$ 1420 Multilabel Counter (PerkinElmer Life Sciences, Boston, MA) and expressed as fold increase on the basal level (DMSO-treated cells).

Measurement of ROS production

Intracellular ROS production was assessed using DCFH-DA. DCFH-DA is a peroxide-sensitive fluorescent probe that is nonpolar and diffuses into the cell. Intracellular esterases cleave the diacetate ester group and entrap the polar, nonfluorescent DCFH within the cell. ROS can oxidize this substance to the fluorescent compound DCF. After the indicated treatments, 5×10^5 cells were incubated in RPMI1640 containing 50 μM DCFH-DA for 30 minutes prior to ROS measurement. Samples incubated with hydrogen peroxide (100 mM) were used as positive controls. The fluorescence was measured with FACSCalibur at 588 nm emission.

Immunofluorescent staining of apoptosis-inducing factor (AIF)

After treatment, 2 to 4×10^4 cells were spun down onto slides, fixed with 4% paraformaldehyde in PBS for 60 minutes, permeabilized with 0.1% sodium dodecyl sulfate (SDS; Nacalai) in PBS for 10 minutes, and blocked with 10% FBS in PBS for 20 minutes. For the simultaneous staining of the nucleus and AIF protein, the cells were labeled with monoclonal mouse anti–poly(adenosine diphosphate–ribose) polymerase (PARP) antibody (1:100 dilution, clone 7D3-6; Pharmingen, San Diego, CA) and polyclonal
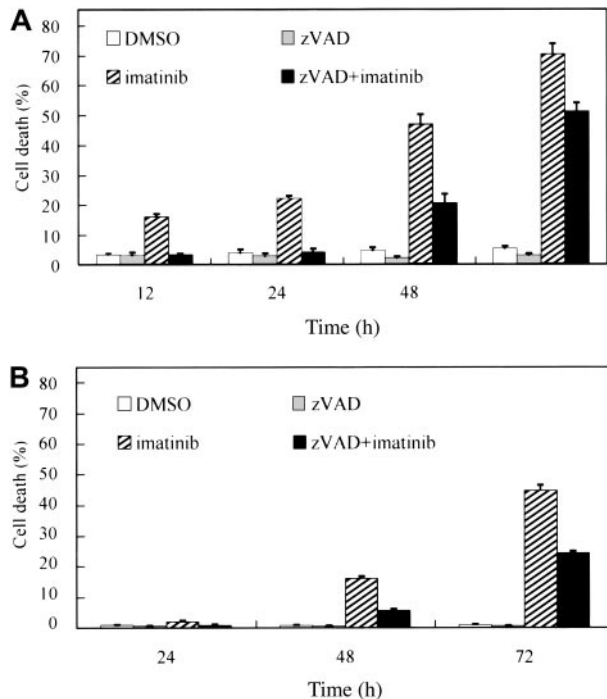
Figure 1. zVAD fails to prevent imatinib-induced cell death. BV173 cells (A) and K562 cells (B) were preincubated with 0.1% DMSO or 40 μM zVAD and subsequently treated with or without 1 μM imatinib for the indicated times. The PI-positive dead cells were determined by flow cytometry. Data represent means ± SEM of 4 individual experiments.

rabbit anti-AIF antibody (1:250 dilution, clone H-300; Santa Cruz Biotechnology, Santa Cruz, CA), followed by secondary staining with cyanin 3 (Cy3)–conjugated goat anti–mouse immunoglobulin G (IgG, 1:100 dilution; Jackson ImmunoResearch, West Grove, PA) and AlexaFluor 488–conjugated goat anti–rabbit IgG (1:200 dilution; Molecular Probes), and observed by fluoroscopy. Every step was performed at room temperature.

Subcellular fractionation and Western blotting

The mitochondria-poor cytosol was obtained by the nitrogen cavitation procedure, which was modified from a previous report.[36] Briefly, after treatment, 3×10^7 cells were washed and resuspended in 1 mL isotonic buffer (250 mM sucrose, 20 mM HEPES-KOH [N-2-hydroxyethylpiperazine-N′-2-ethanesulfonic acid, pH 7.5], 10 mM KCl, 1.5 mM MgCl₂, 1 mM EDTA [ethylenediaminetetraacetic acid], 1 mM EGTA [ethylene glycol tetraacetic acid], 1 mM dithiothreitol [DTT], and protease inhibitors), packed into a Parr 4639 Cell Disruption Bomb (Parr, Moline, IL) at a nitrogen pressure of 100 to 200 psi (1 atmosphere = ~ 14.7 psi, at sea

level), and slowly released into the atmosphere. Following the nitrogen cavitation, unbroken cells and nuclei were removed by centrifugation (at 700g, 5 minutes, 4°C, 2 times). After a further centrifugation (at 10 000g, 15 minutes, 4°C), the supernatant was ultracentrifuged (at 100 000g, one hour, 4°C) to generate the mitochondria-poor cytosol. Cytosolic protein extract (30 μg) was boiled in SDS sample buffer (67 mM Tris [tris(hydroxymethyl)aminomethane, pH 6.8], 2% SDS, 0.03% bromophenol blue, 3% [vol/vol] β-mercaptoethanol, 10% glycerol) for 3 minutes, resolved on 15% SDS–polyacrylamide gel electrophoresis (PAGE) gel (Bio-Rad, Hercules, CA), and transferred onto a polyvinylidene difluoride membrane (Millipore, Bedford, MA). After overnight blocking with 5% nonfat dry milk at room temperature, the membrane was incubated with rabbit polyclonal anti-HtrA2 antibody (kindly provided by Dr Suzuki) for one hour, washed 3 times with TBS-T solution (0.1% Tween 20 in Tris-buffered saline [TBS], pH 7.5), and incubated with horseradish peroxidase–conjugated anti–rabbit IgG antibody (Santa Cruz) for one hour. Blocking and incubations with primary and secondary antibodies were all performed at room temperature. The membrane was washed and bound antibodies were visualized with an enhanced chemiluminescence detection system as specified by the manufacturer (Amersham, Arlington Heights, IL). After stripping the membrane in stripping buffer (62.5 mM Tris-HCl [pH 6.7], 2% SDS, 100 mM 2-mercaptoethanol) for 30 minutes at 56°C, it was reprobed with anti–β-actin antibody (Sigma) to assess the comparability of the protein loading. Intensity of Omi/HtrA2 bands was evaluated using ATTO Lane & Spot Analyzer version 6.0 software (Atto Bioscience, Rockville, MD) and compared with the intensity of the corresponding β-actin bands on the same membrane.

Whole cell lysate was analyzed by the same Western blotting procedure using anti-ABL antibody (Pharmingen) or antiphosphotyrosine antibody (Santa Cruz).

Statistical analysis

Values are expressed as means ± SEM. To evaluate the difference in means between 2 groups, the Mann-Whitney U test was used. StatView-J version 4.5 software (SAS Institute, Cary, NC) was used for all statistical analyses and significance was defined as a P value less than .05.

Results

Inhibition of caspases fails to prevent the imatinib-induced cell death

To confirm caspase dependency in the imatinib-induced cell death of BCR-ABL–positive human leukemic cells, BV173 cells and K562 cells were preincubated with DMSO or zVAD and subsequently treated with or without imatinib. After treatment with imatinib alone, the percentage of PI-positive cells (dead cells)
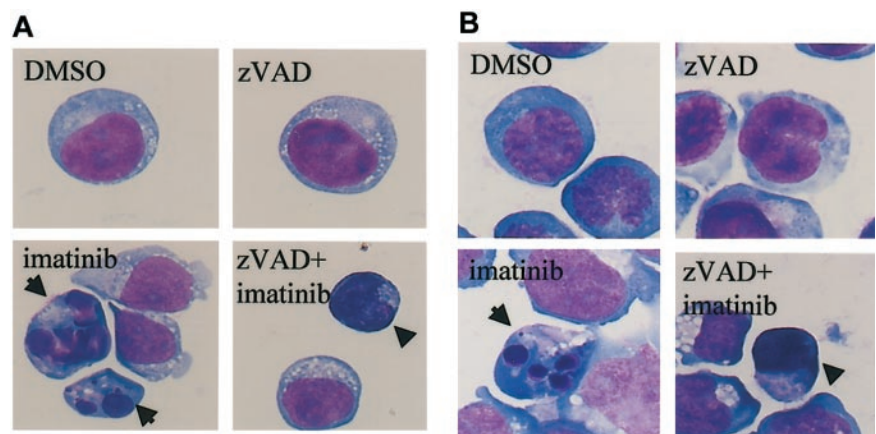

Figure 2. Imatinib induces classical apoptosis, while zVAD + imatinib induces atypical cell death. Diff-Quick–stained cytocentrifuge specimens of BV173 cells (A) and K562 cells (B). BV173 cells and K562 cells were treated for 12 hours and 48 hours, respectively, with DMSO, zVAD, imatinib, and zVAD + imatinib. After treatment with imatinib, BV173 cells and K562 cells exhibited cell shrinkage, nuclear condensation, and nuclear fragmentation, which are characteristic of apoptosis. In contrast, after treatment of zVAD + imatinib, BV173 cells and K562 cells exhibited cell shrinkage, nonfragmented nuclei, and marked cellular pyknosis. Results are representative of 5 individual experiments. Arrows indicate apoptotic cells; arrowheads, atypical cells. Original magnification, × 1000.

Table 1. Apoptotic cell death and atypical cell death are mutually exclusive

	DMSO, %			zVAD, %			Imatinib, %			zVAD + imatinib, %		
	3 hours	6 hours	12 hours	3 hours	6 hours	12 hours	3 hours	6 hours	12 hours	3 hours	6 hours	12 hours
Intact	98.3 ± 0.5	98.3 ± 0.5	98.4 ± 0.1	99.8 ± 0.1	99.8 ± 0.1	99.6 ± 0.1	95.3 ± 0.4	94.4 ± 0.6	90.6 ± 0.3	99.8 ± 0.1	97.2 ± 0.4	93.3 ± 0.6
Apoptotic	1.8 ± 0.5	1.5 ± 0.6	1.4 ± 0.1	< 0.1	< 0.1	< 0.1	4.8 ± 0.4	5.3 ± 0.7	8.2 ± 0.5	< 0.1	< 0.1	< 0.1
Atypical	< 0.1	< 0.1	< 0.1	< 0.1	< 0.1	< 0.1	< 0.1	< 0.1	< 0.1	< 0.1	2.8 ± 0.3	6.6 ± 0.6

Quantitative data were obtained from cytospin specimens of BV173 cells treated with the indicated agents for 3, 6, and 12 hours. "Apoptotic cells" are defined by nuclear fragmentation and chromatin condensation, while "atypical cells" are defined by marked cellular pyknosis, round and shrinked morphology, and a lack of nuclear fragmentation. In imatinib-treated cells, the apoptotic cells appeared as early as 3 hours after treatment and increased thereafter. In zVAD + imatinib-treated cells, the atypical cells appeared later at 6 hours. Of note, the atypical cells were absent in imatinib-treated cells, and the apoptotic cells were absent in zVAD + imatinib-treated cells. Values indicate the percentage of each morphologic type. Data represent means $\pm$ SEM of 4 individual experiments.

increased in a time-dependent fashion both in BV173 cells (Figure 1A; $70.5 \pm 3.3\%$ after 72 hours) and in K562 cells (Figure 1B; $44.7 \pm 1.8\%$ after 72 hours). Unexpectedly, however, the dead cells also increased after treatment with zVAD + imatinib both in BV173 cells (Figure 1A; $51.3 \pm 2.7\%$ after 72 hours) and in K562 cells (Figure 1B; $24.2 \pm 0.7\%$ after 72 hours), although the appearance of dead cells was slightly delayed compared with that in imatinib-treated cells. Importantly, neither DMSO nor zVAD was cytotoxic and, as shown later, the concentration of zVAD was sufficiently high to inhibit the caspase activities throughout these experiments.

Imatinib induces classical apoptosis, while zVAD + imatinib induces atypical cell death

The results shown in Figure 1 suggested the existence of caspase-independent cell death in zVAD + imatinib–treated cells. To determine whether this mode of cell death is apoptosis or not, we performed a morphologic evaluation by light microscopy in the early phase of cell death. In imatinib-treated BV173 cells, apoptotic cells characterized by cell shrinkage, nuclear condensation, and nuclear fragmentation (Figure 2A) began to appear after 3 hours and increased up to $8.2 \pm 0.5\%$ after 12 hours (Table 1). In zVAD + imatinib–treated BV173 cells, such apoptotic cells were barely detectable. Instead, dying cells exhibited an atypical morphology with cellular pyknosis and a lack of nuclear fragmentation (Figure 2A). Such cells appeared after 6 hours and amounted to $6.6 \pm 0.6\%$ after 12 hours (Table 1). The morphologic features of imatinib-treated or zVAD + imatinib–treated K562 cells (Figure 2B) were similar to those of BV173 cells. To discriminate the ultrastructural differences between the apoptotic and the atypical cells, we assessed them using transmission electron microscopy. DMSO-treated control cells exhibited normal morphology characterized by a wavy surface, fine texture of nuclear chromatin, and tubular structure of mitochondria with clearly delineated cristae (Figure 3A). Imatinib-treated apoptotic cells exhibited a smoothing of the cell surface, nuclear fragmentation, compaction and segregation of chromatin into crescents adjacent to the nuclear envelope, mitochondria with obscure cristae, and autolysosomes that incorporated the degenerate mitochondria (Figure 3C). In the later phase, these cells exhibited cell swelling or rupture of the cytoplasmic membrane (Figure 3E), a feature typical for secondary necrosis. In contrast, zVAD + imatinib–treated atypical cells exhibited cell shrinkage, electron-dense nucleus and cytoplasm, chromatin clustering to speckles, lack of nuclear fragmentation, and cytoplasmic vacuoles (Figure 3D). Rupture of the cytoplasmic membrane and mitochondrial swelling were observed thereafter (Figure 3F). Altogether, these ultrastructural alterations are pathognomonic of necrosis, which develops in 2 steps. "Early necrosis" is characterized by several morphologic features of necrosis without disruption

of cytoplasmic membrane and "end-stage necrosis" culminates in the loss of viability.

Internucleosomal DNA fragmentation and decrease in DNA content are observed in imatinib-treated cells, but not in zVAD + imatinib–treated cells

To further characterize the nuclei of these 2 modes of cell death, we examined internucleosomal DNA fragmentation and DNA content. As expected, imatinib-treated cells exhibited internucleosomal DNA fragmentation (Figure 4A) and a subdiploid DNA content (Figure 4B), consistent with their apoptotic morphology (4.8%, 5.3%, and 8.2% at 3, 6, and 12 hours, respectively; Table 1). In contrast, zVAD + imatinib–treated cells exhibited neither internucleosomal DNA fragmentation nor any decrease in DNA content even after 12 hours (Figure 4A-B), when the percentage of atypical cells reached 6.6% (Table 1). These signs of atypical cell death induced by zVAD + imatinib treatment were consistent with the necrotic mode of cell death.
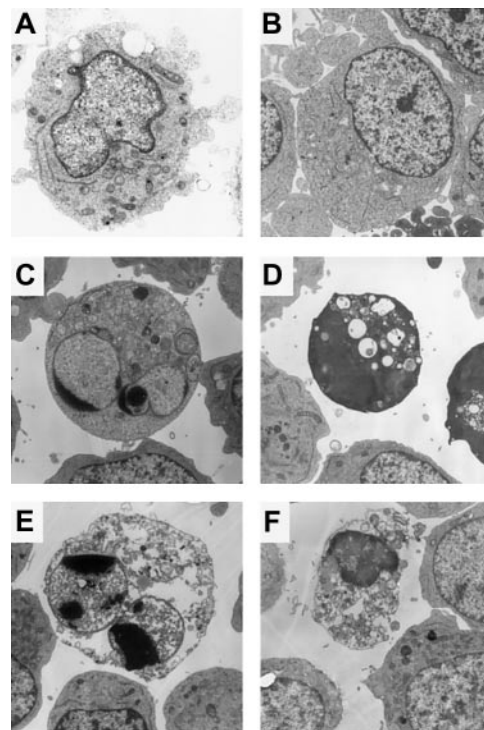

Figure 3. Atypical cell death exhibited necrotic morphology by ultrastructural examination. BV173 cells were treated with DMSO (A), zVAD (B), imatinib (C, E), and zVAD + imatinib (D, F) for 12 hours (A-D) and 48 hours (E-F). Specimens were prepared for transmission electron microscopy as described in "Materials and methods." Results are representative of 3 individual experiments. Original magnification, $\times$ 3000.

Figure 4. Internucleosomal DNA fragmentation and decrease in DNA content are not observed in zVAD + imatinib–induced atypical cell death. BV173 cells were treated with DMSO, imatinib, and zVAD + imatinib for 3, 6, and 12 hours, followed by internucleosomal DNA fragmentation assay and DNA content assay ("Materials and methods"). Internucleosomal DNA fragmentation (A) and decrease in DNA content (B) were observed and augmented in a time-dependent fashion in imatinib-treated cells, whereas neither was observed in zVAD + imatinib–treated cells. M indicates 100–base pair ladder molecular-weight standard; C, control. Values in B indicate the percentage of sub-G_1 fraction. Results are representative of 3 individual experiments.
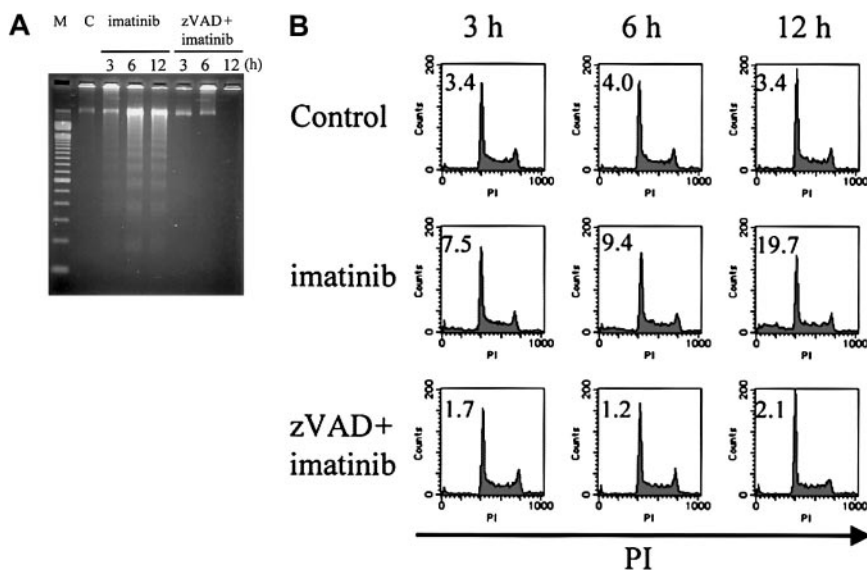
The activation of caspase-9/caspase-3 is involved in imatinib-induced apoptosis, while caspase activities are completely inhibited in zVAD + imatinib–induced necrosis

As previously described,[8-12] imatinib induces the mitochondrial apoptotic pathway, which causes the release of cytochrome c into the cytosol, followed by the activation of caspase-9 and caspase-3. To examine whether this is also the case in our system and to confirm that caspases are completely inhibited after zVAD preincubation, we measured the caspase activities using fluorogenic substrates. As expected, in imatinib-treated cells, caspase-3 and caspase-9 were significantly activated after treatment for 3 hours (Figure 5), confirming the activation of the mitochondrial apoptotic pathway by imatinib. Importantly, in zVAD + imatinib–treated cells, the activities of caspase-3, -8, and -9 were all constantly maintained at or below the control level throughout the experiments (Figure 5).

Loss of mitochondrial transmembrane potential ($\Delta\Psi$m) is observed in the early phase of necrosis

Because the loss of $\Delta\Psi$m represents mitochondrial dysfunction and involvement in cell death,[37-41] we examined the change in $\Delta\Psi$m during necrosis by means of the $\Delta\Psi$m-sensitive fluorochrome DiOC6(3). After treatment with imatinib or zVAD + imatinib, cells were incubated with DiOC6(3) and PI, followed by cytofluorometric analysis. Viable cells exhibited a DiOC6(3)^{high} and

PI^- phenotype, dying cells with a loss of $\Delta\Psi$m were found in DiOC6(3)^{low} and PI^- fraction, and dead cells were DiOC6(3)^{low} and PI^+. As shown in Figure 6, imatinib-treated or zVAD + imatinib–treated BV173 cells (A) and K562 cells (B) exhibited an increase of the DiOC6(3)^{low} and PI^- fraction before the increase of DiOC6(3)^{low} and PI^+ population. Thus, during zVAD + imatinib–triggered necrosis as well as imatinib-triggered apoptosis, the $\Delta\Psi$m dissipation preceded the disruption of plasma membrane integrity.

Neither the overproduction of ROS nor the nuclear translocation of AIF is required for the execution of necrosis, while Omi/HtrA2 is released into the cytosol during necrosis

The results shown in Figure 6 suggest the involvement of mitochondria in necrosis. There are some mediators of caspase-independent cell death in association with mitochondrial dysfunction: overproduction of ROS, nuclear translocation of AIF or Endo G, and release of serine protease Omi/HtrA2 into the cytosol. Because Endo G causes internucleosomal DNA fragmentation,[42] we ruled out the possibility that Endo G was the mediator in our system. Thus we examined the involvement of ROS, AIF, and Omi/HtrA2 in caspase-independent cell death in parallel with that in apoptosis. First, we measured intracellular ROS production after treatment with imatinib or zVAD + imatinib for 3, 6, and 12 hours. Intracellular ROS production did not change after 3 and 6 hours and slightly decreased after 12 hours compared with that in control
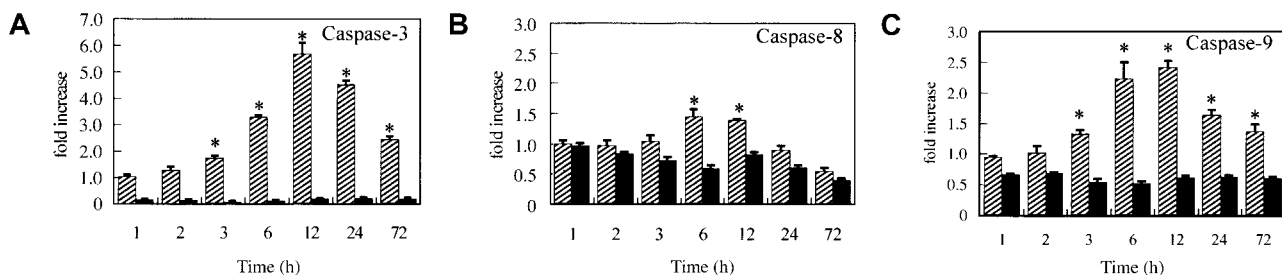

Figure 5. Mitochondrial caspase signaling works in imatinib-treated cells, while caspases are completely inhibited in zVAD + imatinib–treated cells. BV173 cells were treated with DMSO (control), imatinib (hatched bars), and zVAD + imatinib (black bars) for 1, 2, 3, 6, 12, 24, and 72 hours, followed by caspase activity assay ("Materials and methods"). In imatinib-treated cells, significant activation of caspase-9 and caspase-3 preceded that of caspase-8. In zVAD + imatinib–treated cells, all these caspases were inhibited below the control level throughout the experiments. Results are expressed as fold increase compared with control. Data represent means ± SEM of 4 individual experiments. * indicates P is less than .05.
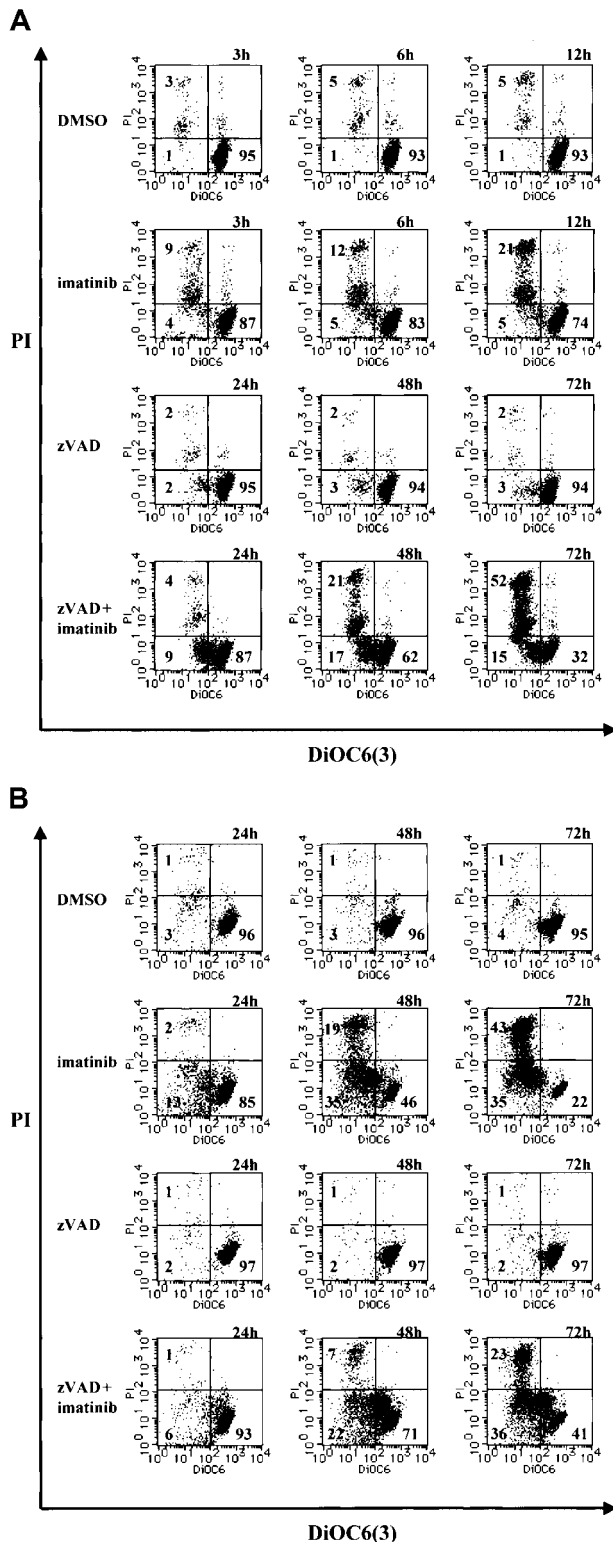
A

B

Figure 6. Mitochondrial transmembrane potential (ΔΨm) is lost in the early phase of necrosis. (A) BV173 cells were treated with DMSO or imatinib for 3, 6, and 12 hours and treated with zVAD or zVAD + imatinib for 24, 48, and 72 hours. (B) K562 cells were treated with DMSO, imatinib, zVAD, and zVAD + imatinib for 24, 48, and 72 hours. These cells were followed by incubation with DiOC6(3) and PI. ΔΨm and cell death were determined by dual-parameter flow cytometry. Results are representative of 4 individual experiments.

(Figure 7A). These results support the others' finding that BCR-ABL directly induces ROS production that is blocked by imatinib.[43] Second, nuclear translocation of AIF was determined by immunofluorescent staining. The localization of AIF in zVAD +

imatinib–treated cells was demonstrated only in the cytoplasm (or mitochondria), not in the nuclei, after 12 hours, while staurosporine-treated cells (as a positive control) showed the nuclear AIF (Figure 7B), as has already been described.[44,45] Also, AIF was not localized to the fragmented nuclei of apoptotic cells. Moreover, subcellular fractionation followed by Western blotting showed that the cytosolic release of AIF was absent both in imatinib-treated cells and in zVAD + imatinib–treated cells (Figure 7C). Finally, we examined the release of Omi/HtrA2 into the cytosol. We found that Omi/HtrA2 was released into the cytosol of imatinib-treated apoptotic cells after 3 hours and zVAD + imatinib–treated necrotic cells after 12 hours (Figure 7C). Mitochondrial contamination was ruled out by the absence of cytochrome oxidase in the cytosol. Using densitometry and correction against β-actin expression, the amount of cytosolic Omi/HtrA2 in imatinib- or zVAD + imatinib–treated cells after 12 hours was found to be increased 2-fold (imatinib) or 1.7-fold (zVAD + imatinib) compared with that in control cells (Figure 7C). Quantitative analysis indicated that the amount of cytosolic Omi/HtrA2 was concordant with the percentage of dying cells in morphologic evaluation (Table 1). In addition, we showed that the direct kinase inhibitory activity of imatinib is equivalent in cells treated with imatinib alone or with imatinib plus additional agents by direct measurement of BCR-ABL phosphotyrosine content and ruled out the possibility that the additional agents directly altered imatinib cellular uptake or activity (Figure 7D).

Trypsinlike serine protease is required for the execution of necrosis

Others have already reported that extramitochondrially overexpressed mature HtrA2 induces caspase-independent cell death and that this death-inducing activity is dependent on the trypsinlike serine protease activity of HtrA2.[46] To further elucidate the role of serine protease in the caspase-independent necrosis, we used 2 serine protease inhibitors, TLCK and TPCK. TLCK is a trypsinlike serine protease inhibitor, while TPCK is a chymotrypsin-like serine protease inhibitor. These agents prevented the zVAD + imatinib–induced necrosis in a dose-dependent fashion (data not shown), with maximal prevention at the indicated concentration of TLCK or TPCK (Figure 8A-B). The cytoprotective effect of TLCK and TPCK was evident both in the early phase (Figure 8A) and in the late phase (Figure 8B-C) of cell death. After treatment for 12 hours, none of the TLCK (or TPCK) + zVAD + imatinib–treated cells exhibited necrotic morphology (Figure 8A). A significant difference in the percentage of dead cells between zVAD + imatinib–treated and TLCK (or TPCK) + zVAD + imatinib–treated cells was seen after treatment for 48 (not shown) and 72 hours, and the preventive effect was greater using TLCK than TPCK both in BV173 cells and in K562 cells (Figure 8B). In addition, these serine protease inhibitors also prevented the loss of ΔΨm, indicated by a relative decrease in the DiOC6(3)^{low} and PI$^-$ fraction of TLCK (or TPCK) + zVAD + imatinib–treated cells compared with that of zVAD + imatinib–treated cells (Figure 8B). Finally, we found that TLCK (or TPCK, not shown) did not prevent the imatinib-induced apoptotic pathway but prevented the zVAD + imatinib–induced necrosis-like PCD pathway (Figure 8C), indicating that these 2 pathways are independent of each other.

Discussion

This is the first report showing that imatinib induces caspase-independent necrosis-like cell death in BCR-ABL–positive cells. It has

Figure 7. Omi/HtrA2 is the only candidate mediator of necrosis. (A) BV173 cells were treated with the indicated agents for 3, 6, and 12 hours, followed by measurement of the intracellular ROS production by DCFH-DA. Dotted contours indicate DMSO-treated cells (as a basal control); bold contours, DMSO-treated, H_2O_2-added cells (as a positive control); filled-in contours, imatinib-treated (upper panel) or zVAD + imatinib–treated (lower panel) cells; and thin contours, autofluorescence (without DCFH-DA). Results are representative of 3 individual experiments. (B) BV173 cells were treated with the indicated agents for 6 hours (STS), or 12 hours (DMSO, imatinib, zVAD + imatinib), followed by immunofluorescent staining of AIF and PARP. Results are representative of 3 individual experiments. (C) BV173 cells were treated with DMSO, zVAD, imatinib, and zVAD + imatinib for the indicated times. Release of AIF and Omi/HtrA2 into the cytosol was assessed by Western blotting following subcellular fractionation. Left 6 bands are the cytosolic fractions, and M indicates the mitochondrial fraction. Each value indicates fold increase in the intensity of the Omi/HtrA2 band on the basal level (imatinib vs DMSO, and zVAD + imatinib vs zVAD [underlined]). Results are representative of 3 individual experiments. (D) BV173 cells were treated with the indicated agents for 3 hours, and each whole cell lysate was assessed by Western blotting. The direct kinase inhibitory activity of imatinib was equivalent in cells treated with imatinib alone or with imatinib plus additional agents.
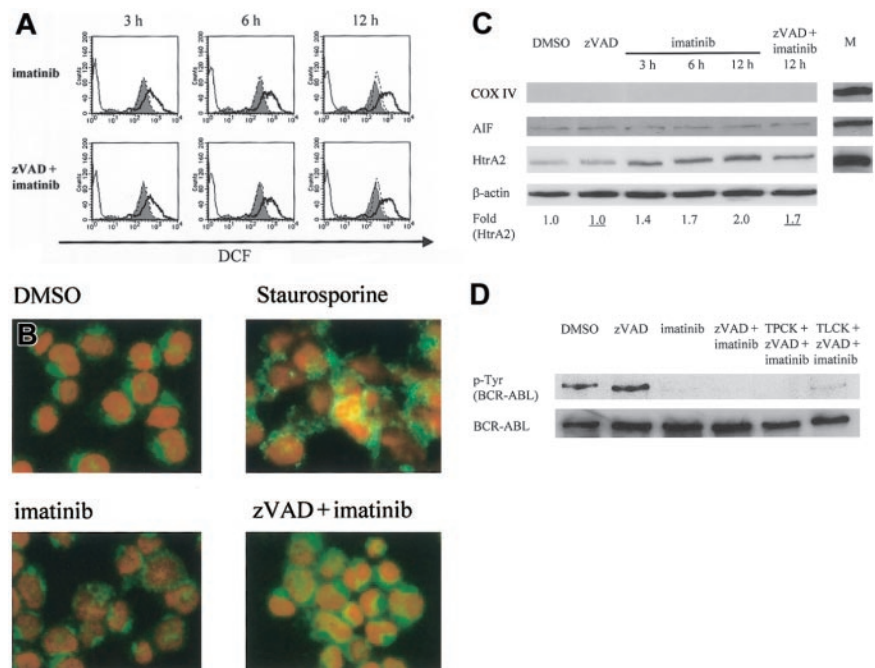
been reported that imatinib induces caspase-dependent apoptosis in BCR-ABL–positive cells, but the present data demonstrate that a broad caspase inhibitor, zVAD, failed to prevent the imatinib-induced cell death and that dying and dead cells exhibited necrotic morphology. Previous reports that showed that zVAD prevented imatinib-induced cell death[3,11,12] did not extensively analyze the mode or the time-course of cell death. The quantification of cell death often relies on the assessment of nuclear fragmentation, internucleosomal DNA fragmentation, and phosphatidylserine exposure on the plasma membrane. This methodology might favor overlooking necrosis or caspase-independent cell death for 2 different reasons. First, necrotic cells do not exhibit nuclear or DNA fragmentation and do not necessarily turn Annexin V–positive in the early phase of cell death.[47] In the absence of thorough morphologic evaluation by light or electron microscopy early necrotic cells may appear "normal."[33,48] Second, inhibition of caspases by zVAD often delays the manifestation of cell death.[26] In the absence of kinetic follow-up studies, this creates the impression that zVAD "inhibits" cell death (when, in reality, it delays cell death). Our data are consistent with a number of reports suggesting that zVAD fails to prevent cell death or even increases the sensitivity of cells to necrosis. In Jurkat cells, zVAD

fails to prevent cell death induced by Bax[49] or by oligomerization of Fas-associated death domain.[31] In human neutrophils[50,51] and L929 cells,[30] zVAD fails to prevent tumor necrosis factor α–induced apoptosis and increases necrosis. In mouse thymocytes, zVAD prevents apoptosis induced by the mitochondrial permeability transition inducers protoporphyrin IX or the carbonyl cyanide m-chlorophenylhydrazone, while thymocytes themselves undergo necrosis.[48] In these reports, necrosis was confirmed by electron microscopic analysis, and the following features were observed: cytoplasmic vacuolation,[49] distension of the mitochondria, and dilatation of the nuclear envelope internal space.[48] However, to our knowledge, there have been no reports on atypical cell death characterized by electron-dense nucleus and cytoplasm and chromatin clustering to speckles as seen in our zVAD + imatinib–treated cells.

The second novel point in the present study is that the serine protease Omi/HtrA2 is likely to be involved in caspase-independent necrosis-like cell death. The modes of caspase-independent cell death are classified into apoptosis-like PCD and necrosis-like PCD, and their mechanisms are often mediated by mitochondria-associated factors such as ROS, AIF, Endo G, and
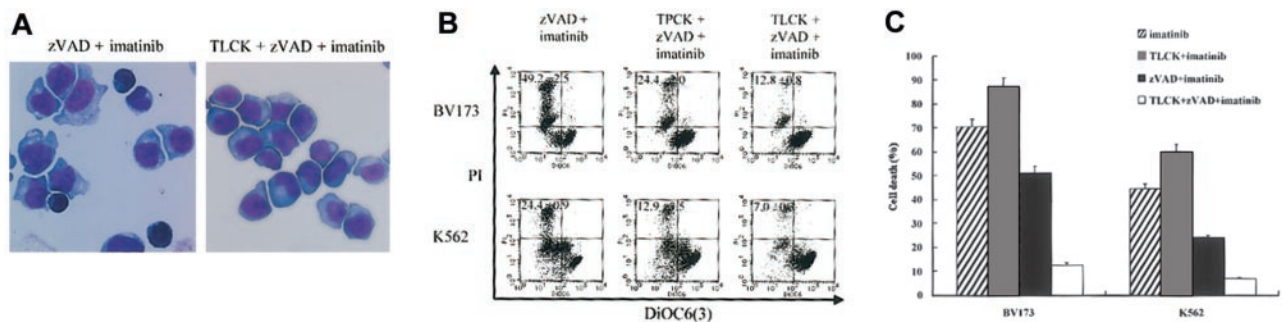
Figure 8. Trypsinlike serine protease is required for the execution of necrosis. (A) BV173 cells were treated with zVAD + imatinib and TLCK + zVAD + imatinib for 12 hours, followed by morphologic evaluation of cytospin specimens. Original magnification, × 1000. (B-C) BV173 cells and K562 cells were treated with the indicated agents for 72 hours, followed by incubation with DiOC6(3) and PI, and analysis by dual-parameter flow cytometry. The concentrations of TLCK and TPCK were as follows: 100 μM and 25 μM for BV173 cells, 200 μM and 50 μM for K562 cells. (B) Values indicate the percentage of the DiOC6(3)^low and PI^+ populations. (C) Cell death is the percentage of the PI^+ populations. Data represent means ± SEM of 4 individual experiments. Striped bars indicate imatinib; gray bars, TLCK + imatinib; black bars, zVAD + imatinib; and white bars, TLCK + zVAD + imatinib.

Omi/HtrA2.[29] Our study demonstrated that imatinib-induced, caspase-independent necrosis was associated with the release of Omi/HtrA2 from mitochondria, yet was not coupled to the overproduction of ROS, nuclear translocation of AIF, or the Endo G–mediated internucleosomal DNA fragmentation. Omi/HtrA2 is a serine protease that is localized in the mitochondrial intermembrane space.[46,52-55] During apoptosis, Omi/HtrA2 is released into the cytosol and inhibits IAPs, thereby deinhibiting the activation of the caspase cascade. In addition, the serine protease activity of Omi/HtrA2 induces caspase-independent cell death with atypical morphologic changes: cell rounding and shrinkage not accompanied by membrane blebbing, apoptotic body formation, or nuclear morphologic changes.[46] These morphologic features seemed similar to those of the caspase-independent necrosis in our study. Additionally, the release of Omi/HtrA2 was not inhibited by zVAD. These findings raised the possibility that Omi/HtrA2 might play a crucial role in zVAD + imatinib–induced necrosis.

TLCK and TPCK are used as serine protease inhibitors as previously described.[56-58] TLCK is a trypsinlike serine protease inhibitor, while TPCK is a chymotrypsin-like serine protease inhibitor. Omi/HtrA2 possesses trypsinlike serine protease activity, thereby inducing atypical cell death.[46] In our study, the caspase-independent necrosis was prevented by these serine protease inhibitors. Moreover, the trypsinlike serine protease inhibitor TLCK showed a greater effect than the chymotrypsin-like TPCK, corroborating that the caspase-independent necrosis was mediated by the trypsinlike serine protease activity of Omi/HtrA2. We considered this mode of cell death as a programmed one in the sense that it was mediated by an inherent cellular protein. In addition, TLCK (or TPCK) + zVAD + imatinib–treated cells exhibited the same degree of growth arrest as zVAD + imatinib–treated cells (not shown), indicating that the serine protease activity was not rate-limiting for the zVAD + imatinib–induced cell cycle block. Both TLCK and TPCK prevented the loss of $\Delta\Psi m$, which is similar to the phenomenon that caspase inhibitors can delay the $\Delta\Psi m$ dissipation and, consequently, cell death.[39] These data indicate that caspases and serine proteases may contribute to the $\Delta\Psi m$ loss and thereby accelerate the cell death. There may be a positive feedback mechanism in the signaling pathway downstream of the mitochondria. On the other hand, there are 2 problems concerning these agents, TLCK and TPCK. First, the trypsinlike serine protease inhibitor TLCK is not necessarily specific for Omi/HtrA2. Therefore, we have not ruled out the possibility that other serine proteases than Omi/HtrA2 might be involved in the caspase-independent necrosis. Second, these 2 agents are alkylating agents as well as serine protease inhibitors.[58] Indeed, in the absence of zVAD, these agents promoted cell death in BV173 cells and K562 cells (Figure 8C). In contrast, in the presence of zVAD, these agents prevented cell death in a dose-dependent fashion. Hence, we considered that, under the inhibition of caspase activities, these agents function as inhibitors of cell death. Accordingly, in order to investigate exactly the role of Omi/HtrA2, it would be more useful to use a specific inhibitor or a dominant-negative form for Omi/HtrA2. Although we tried ucf-101,[59] which has recently been reported to be the specific inhibitor for Omi/HtrA2, this was cytotoxic to our cell lines at the concentration that it inhibited the serine protease activity of Omi/HtrA2. As there is not any specific inhibitor for Omi/HtrA2, others have used general serine protease inhibitors, 4-(2-aminoethyl)-benzenesulfonyl fluoride (AEBSF) and TPCK, and concluded the involvement of Omi/HtrA2 in a p53-dependent apoptosis pathway.[60]

Our result that caspase-independent cell death of BCR-ABL–positive cells exhibits necrotic morphology may be worthy of further investigation. Recently, necrosis has been attracting attention among immunologists and oncologists in terms of therapeutic approaches to cancers. Necrotic cancer cells are ingested by antigen-presenting cells (APCs)[61] and thereby activated APCs in turn induce the immune responses against cancer in vitro[62] and in vivo.[63,64] Moreover, APCs stimulated with necrotic cells display better antitumor activities than those stimulated with apoptotic cells.[62,65,66] These findings suggest that induction of necrosis in cancer cells could constitute a novel maneuver for rendering cancer cells immunogenic. Future investigation will unravel the feasibility of such an "immunotherapy."

In conclusion, our data indicate that imatinib induces caspase-independent, necrosis-like programmed cell death mediated by serine protease activity, most likely by Omi/HtrA2, in BCR-ABL–positive human leukemic cells.

Acknowledgments

References

1. Druker BJ. Inhibition of the Bcr-Abl tyrosine kinase as a therapeutic strategy for CML. Oncogene. 2002;21:8541-8546.

2. Salesse S, Verfaillie CM. BCR/ABL: from molecular mechanisms of leukemia induction to treatment of chronic myelogenous leukemia. Oncogene. 2002;21:8547-8559.

3. Yu C, Krystal G, Varticovksi L, et al. Pharmacologic mitogen-activated protein/extracellular signal-regulated kinase kinase/mitogen-activated protein kinase inhibitors interact synergistically with STI571 to induce apoptosis in Bcr/Abl-expressing human leukemia cells. Cancer Res. 2002;62:188-199.

4. Sonoyama J, Matsumura I, Ezoe S, et al. Functional cooperation among Ras, STAT5, and phosphatidylinositol 3-kinase is required for full oncogenic activities of BCR/ABL in K562 cells. J Biol Chem. 2002;277:8076-8082.

5. Nimmanapalli R, Bhalla K. Novel targeted therapies for Bcr-Abl positive acute leukemias: beyond STI571. Oncogene. 2002;21:8584-8590.

6. Amarante-Mendes GP, McGahon AJ, Nishioka WK, Afar DE, Witte ON, Green DR. Bcl-2-independent Bcr-Abl-mediated resistance to apoptosis: protection is correlated with up regulation of Bcl-xL. Oncogene. 1998;16:1383-1390.

7. Amarante-Mendes GP, Naekyung Kim C, Liu L, et al. Bcr-Abl exerts its antiapoptotic effect against diverse apoptotic stimuli through blockage of mitochondrial release of cytochrome C and activation of caspase-3. Blood. 1998;91:1700-1705.

8. Deininger MW, Goldman JM, Lydon N, Melo JV. The tyrosine kinase inhibitor CGP57148B selectively inhibits the growth of BCR-ABL-positive cells. Blood. 1997;90:3691-3698.

9. Beran M, Cao X, Estrov Z, et al. Selective inhibition of cell proliferation and BCR-ABL phosphorylation in acute lymphoblastic leukemia cells expressing Mr 190,000 BCR-ABL protein by a tyrosine kinase inhibitor (CGP-57148). Clin Cancer Res. 1998;4:1661-1672.

10. Gambacorti-Passerini C, le Coutre P, Mologni L, et al. Inhibition of the ABL kinase activity blocks the proliferation of BCR/ABL+ leukemic cells and induces apoptosis. Blood Cells Mol Dis. 1997;23:380-394.

11. Dan S, Naito M, Tsuruo T. Selective induction of apoptosis in Philadelphia chromosome-positive chronic myelogenous leukemia cells by an inhibitor of BCR-ABL tyrosine kinase, CGP 57148. Cell Death Differ. 1998;5:710-715.

12. Mow BM, Chandra J, Svingen PA, et al. Effects of the Bcr/abl kinase inhibitors STI571 and adaphostin (NSC 680410) on chronic myelogenous leukemia cells in vitro. Blood. 2002;99:664-671.

13. Druker BJ, Talpaz M, Resta DJ, et al. Efficacy and safety of a specific inhibitor of the BCR-ABL tyrosine kinase in chronic myeloid leukemia. N Engl J Med. 2001;344:1031-1037.

14. Druker BJ, Sawyers CL, Kantarjian H, et al. Activity of a specific inhibitor of the BCR-ABL tyrosine kinase in the blast crisis of chronic myeloid leukemia and acute lymphoblastic leukemia with the Philadelphia chromosome. N Engl J Med. 2001; 344:1038-1042.

15. Kantarjian H, Sawyers C, Hochhaus A, et al. Hematologic and cytogenetic responses to imatinib mesylate in chronic myelogenous leukemia. N Engl J Med. 2002;346:645-652.

16. Talpaz M, Silver RT, Druker BJ, et al. Imatinib induces durable hematologic and cytogenetic responses in patients with accelerated phase chronic myeloid leukemia: results of a phase 2 study. Blood. 2002;99:1928-1937.

17. Sawyers CL, Hochhaus A, Feldman E, et al. Imatinib induces hematologic and cytogenetic responses in patients with chronic myelogenous leukemia in myeloid blast crisis: results of a phase II study. Blood. 2002;99:3530-3539.

18. Kantarjian HM, Cortes J, O'Brien S, et al. Imatinib mesylate (STI571) therapy for Philadelphia chromosome-positive chronic myelogenous leukemia in blast phase. Blood. 2002;99:3547-3553.

19. Braziel RM, Launder TM, Druker BJ, et al. Hematopathologic and cytogenetic findings in imatinib mesylate-treated chronic myelogenous leukemia patients: 14 months' experience. Blood. 2002; 100:435-441.

20. Kantarjian HM, O'Brien S, Cortes JE, et al. Imatinib mesylate therapy for relapse after allogeneic stem cell transplantation for chronic myelogenous leukemia. Blood. 2002;100:1590-1595.

21. O'Dwyer ME, Mauro MJ, Kurilik G, et al. The impact of clonal evolution on response to imatinib mesylate (STI571) in accelerated phase CML. Blood. 2002;100:1628-1633.

22. Ottmann OG, Druker BJ, Sawyers CL, et al. A phase 2 study of imatinib in patients with relapsed or refractory Philadelphia chromosome-positive acute lymphoid leukemias. Blood. 2002;100: 1965-1971.

23. Kerr JF, Wyllie AH, Currie AR. Apoptosis: a basic biological phenomenon with wide-ranging implications in tissue kinetics. Br J Cancer. 1972;26: 239-257.

24. Wyllie AH, Morris RG, Smith AL, Dunlop D. Chromatin cleavage in apoptosis: association with condensed chromatin morphology and dependence on macromolecular synthesis. J Pathol. 1984;142:67-77.

25. Hengartner MO. The biochemistry of apoptosis. Nature. 2000;407:770-776.

26. Kitanaka C, Kuchino Y. Caspase-independent programmed cell death with necrotic morphology. Cell Death Differ. 1999;6:508-515.

27. Bursch W. The autophagosomal-lysosomal compartment in programmed cell death. Cell Death Differ. 2001;8:569-581.

28. Proskuryakov SY, Konoplyannikov AG, Gabai VL. Necrosis: a specific form of programmed cell death? Exp Cell Res. 2003;283:1-16.

29. Mathiasen IS, Jaattela M. Triggering caspase-independent cell death to combat cancer. Trends Mol Med. 2002;8:212-220.

30. Vercammen D, Beyaert R, Denecker G, et al. Inhibition of caspases increases the sensitivity of L929 cells to necrosis mediated by tumor necrosis factor. J Exp Med. 1998;187:1477-1485.

31. Kawahara A, Ohsawa Y, Matsumura H, Uchiyama Y, Nagata S. Caspase-independent cell killing by Fas-associated protein with death domain. J Cell Biol. 1998;143:1353-1360.

32. van Loo G, Saelens X, van Gurp M, MacFarlane M, Martin SJ, Vandenabeele P. The role of mitochondrial factors in apoptosis: a Russian roulette

with more than one bullet. Cell Death Differ. 2002; 9:1031-1042.

33. Leist M, Jaattela M. Four deaths and a funeral: from caspases to alternative mechanisms. Nat Rev Mol Cell Biol. 2001;2:589-598.

34. Fleury C, Mignotte B, Vayssiere JL. Mitochondrial reactive oxygen species in cell death signaling. Biochimie. 2002;84:131-141.

35. Rose AL, Smith BE, Maloney DG. Glucocorticoids and rituximab in vitro: synergistic direct antiproliferative and apoptotic effects. Blood. 2002;100: 1765-1773.

36. Gottlieb RA, Adachi S. Nitrogen cavitation for cell disruption to obtain mitochondria from cultured cells. Methods Enzymol. 2000;322:213-221.

37. Zamzami N, Marchetti P, Castedo M, et al. Reduction in mitochondrial potential constitutes an early irreversible step of programmed lymphocyte death in vivo. J Exp Med. 1995;181:1661-1672.

38. Kroemer G, Petit P, Zamzami N, Vayssiere JL, Mignotte B. The biochemistry of programmed cell death. Faseb J. 1995;9:1277-1287.

39. Susin SA, Zamzami N, Kroemer G. Mitochondria as regulators of apoptosis: doubt no more. Biochim Biophys Acta. 1998;1366:151-165.

40. Kroemer G, Reed JC. Mitochondrial control of cell death. Nat Med. 2000;6:513-519.

41. Martinou JC, Green DR. Breaking the mitochondrial barrier. Nat Rev Mol Cell Biol. 2001;2:63-67.

42. Li LY, Luo X, Wang X. Endonuclease G is an apoptotic DNase when released from mitochondria. Nature. 2001;412:95-99.

43. Sattler M, Verma S, Shrikhande G, et al. The BCR/ABL tyrosine kinase induces production of reactive oxygen species in hematopoietic cells. J Biol Chem. 2000;275:24273-24278.

44. Dumont C, Durrbach A, Bidere N, et al. Caspase-independent commitment phase to apoptosis in activated blood T lymphocytes: reversibility at low apoptotic insult. Blood. 2000;96:1030-1038.

45. Susin SA, Lorenzo HK, Zamzami N, et al. Molecular characterization of mitochondrial apoptosis-inducing factor. Nature. 1999;397:441-446.

46. Suzuki Y, Imai Y, Nakayama H, Takahashi K, Takio K, Takahashi R. A serine protease, HtrA2, is released from the mitochondria and interacts with XIAP, inducing cell death. Mol Cell. 2001;8:613-621.

47. Narvaez CJ, Welsh J. Role of mitochondria and caspases in vitamin D-mediated apoptosis of MCF-7 breast cancer cells. J Biol Chem. 2001; 276:9101-9107.

48. Hirsch T, Marchetti P, Susin SA, et al. The apoptosis-necrosis paradox: apoptogenic proteases activated after mitochondrial permeability transition determine the mode of cell death. Oncogene. 1997;15:1573-1581.

49. Xiang J, Chao DT, Korsmeyer SJ. BAX-induced cell death may not require interleukin 1 beta-converting enzyme-like proteases. Proc Natl Acad Sci U S A. 1996;93:14559-14563.

50. Liu CY, Takemasa A, Liles WC, et al. Broad-spectrum caspase inhibition paradoxically augments cell death in TNF-alpha-stimulated neutrophils. Blood. 2003;101:295-304.

51. Maianski NA, Roos D, Kuijpers TW. Tumor necrosis factor alpha induces a caspase-independent death pathway in human neutrophils. Blood. 2003;101:1987-1995.

52. van Loo G, van Gurp M, Depuydt B, et al. The serine protease Omi/HtrA2 is released from mitochondria during apoptosis: Omi interacts with caspase-inhibitor XIAP and induces enhanced caspase activity. Cell Death Differ. 2002;9:20-26.

53. Hegde R, Srinivasula SM, Zhang Z, et al. Identification of Omi/HtrA2 as a mitochondrial apoptotic serine protease that disrupts inhibitor of apoptosis protein-caspase interaction. J Biol Chem. 2002;277:432-438.

54. Martins LM, Iaccarino I, Tenev T, et al. The serine protease Omi/HtrA2 regulates apoptosis by binding XIAP through a reaper-like motif. J Biol Chem. 2002;277:439-444.

55. Verhagen AM, Silke J, Ekert PG, et al. HtrA2 promotes cell death through its serine protease activity and its ability to antagonize inhibitor of apoptosis proteins. J Biol Chem. 2002;277:445-454.

56. Huang Y, Sheikh MS, Fornace AJ Jr, Holbrook NJ. Serine protease inhibitor TPCK prevents Taxol-induced cell death and blocks c-Raf-1 and Bcl-2 phosphorylation in human breast carcinoma cells. Oncogene. 1999;18:3431-3439.

57. Mitsui C, Sakai K, Ninomiya T, Koike T. Involvement of TLCK-sensitive serine protease in colchicine-induced cell death of sympathetic neurons in culture. J Neurosci Res. 2001;66:601-611.

58. Cromlish JA, Roeder RG. Human transcription factor IIIC (TFIIIC): purification, polypeptide structure, and the involvement of thiol groups in specific DNA binding. J Biol Chem. 1989;264:18100-18109.

59. Cilenti L, Lee Y, Hess S, et al. Characterization of a novel and specific inhibitor for the pro-apoptotic protease Omi/HtrA2. J Biol Chem. 2003;278: 11489-11494.

60. Jin S, Kalkum M, Overholtzer M, Stoffel A, Chait BT, Levine AJ. CIAP1 and the serine protease HTRA2 are involved in a novel p53-dependent apoptosis pathway in mammals. Genes Dev. 2003;17:359-367.

61. Hirt UA, Gantner F, Leist M. Phagocytosis of non-apoptotic cells dying by caspase-independent mechanisms. J Immunol. 2000;164:6520-6529.

62. Reiter I, Krammer B, Schwamberger G. Cutting edge: differential effect of apoptotic versus necrotic tumor cells on macrophage antitumor activities. J Immunol. 1999;163:1730-1732.

63. Chen Y, Douglass T, Jeffes EW, et al. Living T9 glioma cells expressing membrane macrophage colony-stimulating factor produce immediate tumor destruction by polymorphonuclear leukocytes and macrophages via a "paraptosis"-induced pathway that promotes systemic immunity against intracranial T9 gliomas. Blood. 2002;100: 1373-1380.

64. Gough MJ, Melcher AA, Ahmed A, et al. Macrophages orchestrate the immune response to tumor cell death. Cancer Res. 2001;61:7240-7247.

65. Steinman RM, Turley S, Mellman I, Inaba K. The induction of tolerance by dendritic cells that have captured apoptotic cells. J Exp Med. 2000;191: 411-416.

66. Sauter B, Albert ML, Francisco L, Larsson M, Somersan S, Bhardwaj N. Consequences of cell death: exposure to necrotic tumor cells, but not primary tissue cells or apoptotic cells, induces the maturation of immunostimulatory dendritic cells. J Exp Med. 2000;191:423-434.